Coherent c-axis transport in the underdoped cuprate superconductor YBa$_2$Cu$_3$O$_y$

B. Vignolle,[1] B. J. Ramshaw,[2] James Day,[2] David LeBoeuf,[1] Stéphane Lepault,[1] Ruixing Liang,[2,3] W. N. Hardy,[2,3]
D. A. Bonn,[2,3] Louis Taillefer,[3,4] and Cyril Proust[1,3,*]

[1]*Laboratoire National des Champs Magnétiques Intenses, UPR 3228, (CNRS-INSA-UJF-UPS), Toulouse F-31400, France*
[2]*Department of Physics and Astronomy, University of British Columbia, Vancouver V6T 1Z1, Canada*
[3]*Canadian Institute for Advanced Research, Toronto M5G 1Z8, Canada*
[4]*Département de physique & RQMP, Université de Sherbrooke, Sherbrooke, Québec J1K 2R1, Canada*

The electrical resistivity ρ_c of the underdoped cuprate superconductor YBa$_2$Cu$_3$O$_y$ was measured perpendicular to the CuO$_2$ planes on ultrahigh quality single crystals in magnetic fields large enough to suppress superconductivity. The incoherent insulating-like behavior of ρ_c at high temperature, characteristic of all underdoped cuprates, is found to cross over to a coherent regime of metallic behavior at low temperature. This crossover coincides with the emergence of the small electron pocket detected in the Fermi surface of YBa$_2$Cu$_3$O$_y$ via quantum oscillations, the Hall and Seebeck coefficients, and with the detection of a unidirectional modulation of the charge density as seen by high-field nuclear magnetic resonance measurements. The low coherence temperature is quantitatively consistent with the small hopping integral $t_\perp$ inferred from the splitting of the quantum oscillation frequencies. We conclude that the Fermi-surface reconstruction in YBa$_2$Cu$_3$O$_y$ at dopings from $p = 0.08$ to at least $p = 0.15$, attributed to stripe order, produces a metallic state with three-dimensional coherence deep in the underdoped regime.

PACS number(s): 74.25.Bt, 74.25.Ha

I. INTRODUCTION

Hole-doped cuprate superconductors stand out because of the presence of an enigmatic pseudogap phase in the underdoped regime.[1] From angle-resolved photoemission spectroscopy (ARPES) measurements, the pseudogap is defined by the lack of a well-defined quasiparticle peak in the antinodal region of the Brillouin zone leading to Fermi arcs.[2] Among the peculiar properties in the pseudogap phase, the dichotomy between the insulating-like interplane resistivity along the c axis and the metallic in-plane resistivity down to T_c in many underdoped cuprates is still heavily debated.[3–5] This dichotomy has been considered as strong support of the spin-singlet approach to the pseudogap phase,[6] which considers that coherent charge transport is strictly bidimensional and c-axis resistivity should diverge as $T \to 0$. Among other models that have been proposed, one of these is based on incoherent tunneling between layers assisted by interplanar disorder (see Ref. 7 and references therein). Finally, recent valence-bond dynamical mean-field calculations have established a clear connection between the peculiar c-axis charge transport and the lack of coherent quasiparticles as the pseudogap opens in the antinodal region.[8] This model is in good agreement with c-axis optical conductivity measurements which reveal the absence of a Drude peak at low frequencies in the underdoped normal state above T_c (Ref. 9).

To understand c-axis transport, not only must the Fermi arcs observed by ARPES above T_c be taken into account, but also the observation of quantum oscillations showing that the Fermi surface (FS) of underdoped cuprates undergoes a profound transformation at low temperature.[10] Combined with the negative Hall[11] and Seebeck coefficients[12,13] at low temperature, these measurements demonstrate that the FS of underdoped YBa$_2$Cu$_3$O$_y$ is made of small electron pockets in contrast to the large hole-like FS of the overdoped cuprates.[14] The underlying translational symmetry breaking, which causes the Fermi surface reconstruction, has been observed in high-fields nuclear magnetic resonance (NMR) measurements.[15] These microscopic measurements have revealed that at low temperature and above a threshold magnetic field the translational symmetry of the CuO$_2$ planes in YBa$_2$Cu$_3$O$_y$ is broken by the emergence of a unidirectional modulation of the charge density. This conclusion is supported by a comparative study of thermoelectric transport in underdoped YBa$_2$Cu$_3$O$_y$ and in La$_{1.8-x}$Eu$_{0.2}$Sr$_x$CuO$_4$—a cuprate where stripe order is well established from x-ray diffraction[16]—which argues in favor of a charge stripe order causing reconstruction of the FS at low temperature for $p > 0.08$ (Ref. 13). This charge stripe order can naturally be interpreted as a competing order with superconductivity akin to the smectic stripe phase observed in the archetypal La$_{1.6-x}$Nd$_{0.4}$Sr$_x$CuO$_4$ (Ref. 17).

Here we directly address the consequence of the Fermi surface reconstruction by stripe-charge order on c-axis charge transport by measuring the c-axis resistivity at low temperature in magnetic fields large enough to suppress superconductivity. We found that the c-axis resistivity becomes metallic-like at low temperature, and interpret this as a consequence of c-axis coherence. The low coherence temperature implies a small c-axis dispersion and therefore a small hopping integral $t_\perp$, in quantitative agreement with the splitting of the multiple quantum oscillation frequencies.[18–21] The onset of this crossover coincides with the FS reconstruction leading to the emergence of a high mobility electron pocket which produces metallic-like transport both in the plane and along the c axis. The coherence temperature decreases as the doping level decreases and vanishes at a hole doping $p \approx 0.08$, corresponding to the doping level where the electron pocket disappears.[22]

II. SAMPLE PREPARATION AND EXPERIMENTAL SETUP

The samples studied were single crystals of YBa$_2$Cu$_3$O$_y$, grown in nonreactive BaZrO$_3$ crucibles from high-purity
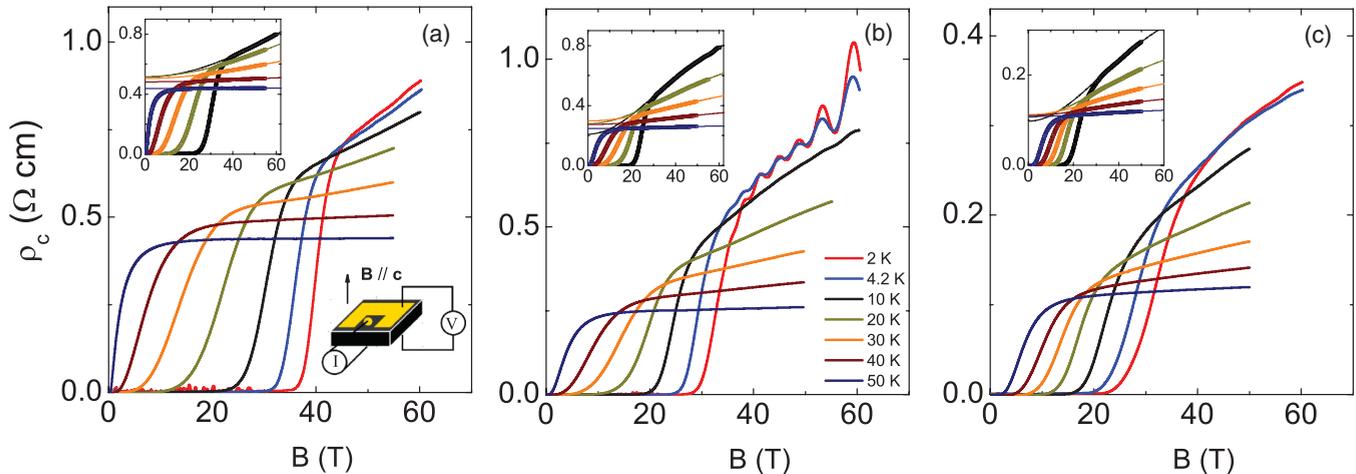
FIG. 1. (Color online) Electrical resistivity ρ_c of $YBa_2Cu_3O_y$ for a current I and a magnetic field B along the c axis ($I \parallel B \parallel c$). Three underdoped samples were measured at different temperatures below T_c (as indicated) in pulsed magnetic fields up to 60 T. The doping level of each sample is (a) $p = 0.097$, (b) $p = 0.109$, and (c) $p = 0.120$. Insets: Same data between 10 and 50 K with a fit of each isotherm (thin solid lines) using a two-band model above the superconducting transition (see Sec. V).

starting materials and subsequently detwinned.[23] The superconducting transition temperatures have been obtained by resistivity measurements at zero field: $T_c = 57.0$ K ($p = 0.097$), $T_c = 61.3$ K ($p = 0.109$), and $T_c = 66.4$ K ($p = 0.120$). The doping p of each crystal was inferred from its superconducting transition temperature T_c (Ref. 24). Electrical contacts to the sample were made by evaporating gold with large current pads and small voltage pads mounted across the top and bottom so as to short out any in-plane current [see inset of Fig. 1(a)]. Several samples with typical dimensions $(1 \times 1 \times t)$ mm^3 of different thicknesses $t = 0.05$–0.15 mm were measured, each giving similar values of the absolute c-axis resistivity. The resistivity was measured at the Laboratoire National des Champs Magnétiques Intenses (LNCMI) in Toulouse, France, in pulsed magnetic fields up to 60 T. A current excitation of 5 mA at $\approx$ 60 kHz was used. The voltage (and a reference signal) was digitized using a high-speed digitizer and postanalyzed to perform the phase comparison.

III. c-AXIS MAGNETORESISTANCE

Figure 1 presents the longitudinal c-axis resistivity up to 60 T for the three underdoped samples of $YBa_2Cu_3O_y$. Below 60 K, a strong positive magnetoresistance (MR) grows with decreasing temperature, in good agreement with earlier high-field measurements[25] of ρ_c on $YBa_2Cu_3O_y$ crystals with $T_c = 60$ K. At very low temperature, quantum oscillations are most clearly seen in the sample with $p = 0.109$ [see Fig. 1(b)] and are just above the noise level for the other two [Figs. 1(a) and 1(c)]. They arise from the quantization of cyclotron orbits perpendicular to the magnetic field. The frequencies and temperature dependence of these oscillations are consistent with previous reports.[10,18–20] Two features common to all three samples are the rise of the in-field c-axis resistivity down to about 4 K, and a tendency to saturation at lower temperature. This behavior is best captured in Fig. 2 where the resistivity is plotted as a function of temperature at

different magnetic fields. As T is lowered, the c-axis resistivity first exhibits insulating behavior, but instead of diverging as $T \to 0$, it crosses over to a regime where it tends to saturate at the lowest temperatures in all three samples.
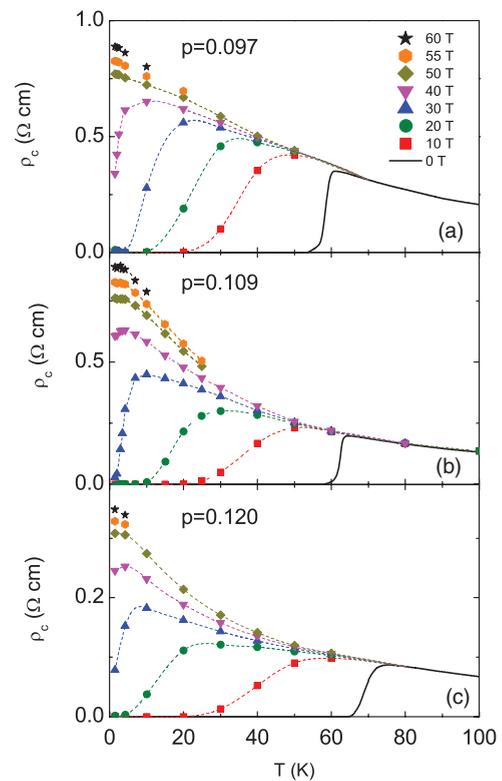
FIG. 2. (Color online) Electrical resistivity ρ_c of $YBa_2Cu_3O_y$ (a) $p = 0.097$, (b) $p = 0.109$, and (c) $p = 0.120$ plotted as a function of temperature for different values of the magnetic field. Dashed lines are a guide to the eye. The increase of the in-field c-axis resistivity down to about 4 K is in part due to the strong magnetoresistance which develops at temperatures below 60 K.

IV. FLUX FLOW CONTRIBUTION TO THE RESISTIVITY

Upon cooling, the resistivity drops because of superconductivity. This drop starts at lower temperature for higher fields. We define the threshold field beyond which the normal state is reached as the field above which $\rho_c(T)$ shows no drop. To confirm that the tendency to saturation of $\rho_c(T)$ at low temperature is not due to some compensation between superconducting drop (as seen for the data below 40 T) and insulating-like normal-state resistivity, we show that the tendency to saturation persists at fields above a threshold field down to the lowest temperatures (see Fig. 2). In all three samples, 50 T is above the threshold field down to the lowest temperatures. Therefore the magnetoresistance measured at 50 T is purely a normal-state property at all three dopings.

The Nernst effect is a sensitive probe of flux flow because moving vortices make a large positive contribution to the Nernst coefficient. In Fig. 3, we compare the field dependence of the Nernst coefficient measured in $YBa_2Cu_3O_y$ at $p = 0.12$ and $T = 10$ K (Ref. 12) [Fig. 3(a)] with that of the in-plane
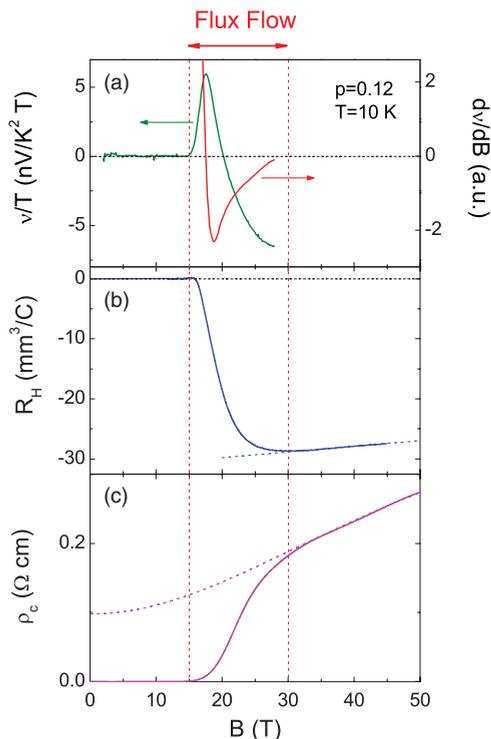
FIG. 3. (Color online) Field dependence of (a) the Nernst coefficient (Ref. 12), (b) the Hall coefficient (Ref. 11), and (c) the c-axis resistivity [Fig. 1(c)] of $YBa_2Cu_3O_y$ at $p = 0.12$ and $T = 10$ K. Above a threshold field of about 30 T (indicated by the right vertical dashed red line), the Nernst coefficient ν [panel (a); green curve] saturates to its negative quasiparticle value, as demonstrated by its derivative [panel (a); red curve] which goes to zero as $B \approx 30$ T. This saturation shows that the positive contribution to the Nernst coefficient from superconducting fluctuations has become negligible above 30 T. Above this field, the Hall coefficient is almost flat [dashed blue line in panel (b)] and the two-band model fit to the c-axis resistivity [dashed magenta line in panel (c)] merges with the data. We conclude that at 10 K and above 30 T the flux-flow contribution to the transport properties is negligible, and the large magnetoresistance at high field is purely a property of the normal state at this doping level.

Hall coefficient[11] [Fig. 3(b)] and c-axis resistivity [Fig. 3(c)]. The Nernst coefficient develops a strong positive peak above the melting line due to vortex motion in the vortex liquid phase and is followed by a gradual descent to negative values (the quasiparticle contribution) until it becomes almost flat as the field approaches 30 T. This saturation is best captured by the field derivative of the Nernst coefficient shown by a red line in Fig. 3(a). Above the threshold field of about 30 T, the Hall coefficient becomes flat [as indicated by the blue dashed line in Fig. 3(b)] and the two-band model used to fit the normal state c-axis resistivity merges with the data [see Fig. 3(c) and Sec. V]. This comparison confirms that flux-flow contribution to the normal-state transport is negligible, that is to say the magnetoresistance is entirely due to quasiparticles, for fields greater than 30 T at $T = 10$ K for $p = 0.120$.

The same conclusion can be drawn for the other samples thanks to Hall effect measurements.[11] The key observation is that $T_0(B)$, the temperature at which $R_H(T)$ changes sign, is independent of field at high fields (from 40 up to 60 T) for samples in the doping range studied here. This shows that the temperature-induced sign change in R_H at high fields is not caused by flux flow and is thus clearly a property of the normal state.

Earlier high-field measurements of ρ_c in $YBa_2Cu_3O_y$ (Ref. 25) show a striking difference between the large magnetoresistance observed in samples with $T_c = 60$ K and the absence of the magnetoresistance in samples with $T_c = 49$ K. This can only be due to normal state transport properties and can be explained by the vanishing of the very mobile electron pocket for the low doping sample.[22] There is no alternative explanation in terms of flux flow.

V. CROSSOVER TOWARDS COHERENT c-AXIS TRANSPORT

In fields of 50 T and above, where the c-axis resistivity tends to saturate as $T \rightarrow 0$, the nonsuperconducting ground state of $YBa_2Cu_3O_y$ is coherent in all three directions at $p = 0.10$–0.12. This behavior is best captured in Fig. 4, where the resistivities for the sample with $p = 0.109$ measured at zero field (solid black line) and at $B = 55$ T (orange symbols) are compared with the insulating-like high temperature behavior, where the c-axis resistivity diverges as $1/T$ (blue solid line).

The observation of c-axis coherent transport means that coherent Bloch bands along the c axis are present at low temperature and that charge carriers are not confined to the CuO_2 planes.[4] Compared to the situation in overdoped cuprate superconductors, where there is no doubt about the existence of a three-dimensional Fermi surface,[26] the c-axis coherent transport in underdoped $YBa_2Cu_3O_y$ appears at low temperature where the FS is reconstructed. NMR measurements performed on the same sample ($p = 0.108$) and in the same temperature/field range where quantum oscillations have been observed,[15] reveal an unidirectional charge stripe order below a temperature $T_{charge} = 50 \pm 10$ K above a threshold field $B \approx 20$ T. Not surprisingly, the transition temperature T_{charge} obtained from NMR measurement coincides roughly with the temperature T_0, the temperature at which $R_H(T)$ changes sign.

In the magnetic field/temperature range where the FS undergoes a reconstruction driven by the charge stripe order, a high
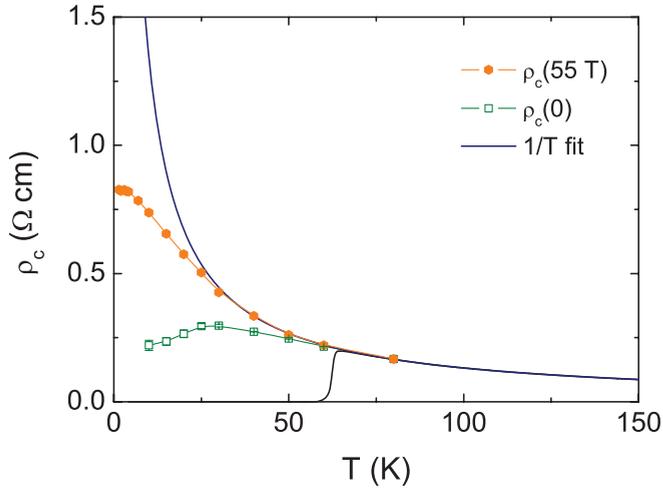
FIG. 4. (Color online) Temperature dependence of the *c*-axis resistivity of $YBa_2Cu_3O_y$ ($p = 0.109$) measured at zero magnetic field (black solid line) and at $B = 55$ T (orange symbols). Blue solid line is a $1/T$ fit to the high temperature data up to 300 K. The saturation of the in-field resistivity at low temperature contrasts with the insulating-like behavior seen at high temperature. The green open squares correspond to the resistivity from which the magnetoresistance has been subtracted using a two-band model to extrapolate the normal-state data of Fig. 1 to $B = 0$ (see Sec. V).

mobility electron pocket dominates the transport properties. Although recent specific heat[27] measurements performed at high fields point to a Fermi surface made of only one pocket per CuO_2 plane,[28] the emergence of a strong non-B^2 MR at low temperature (see Fig. 1) is naturally explained by the FS reconstruction into electron and hole sheets due to the ambipolar character of the Fermi surface. In Fig. 5 we compare the slope of the magnetoresistance $\rho_c(B)$ and the in-plane Hall coefficient R_H as a function of temperature measured at the same hole doping. The onset of the MR in ρ_c coincides with the FS reconstruction thus revealing the two roles played by the electron pocket: it enhances the orbital MR due to in-plane motion of carriers and it allows the MR to be reflected in interplane transport.

To reveal that ρ_c is metallic-like at low temperature it is necessary to obtain the MR-free temperature dependence of $\rho_c(T)$ by extrapolating the in-field resistivity $\rho_c(B)$ to $B = 0$, defined as $\rho_c(0)$. Since a strong MR develops at low temperature, any smooth extrapolation to $B = 0$ will give the same trend for the temperature dependence of $\rho_c(0)$, namely an initial rise with decreasing temperature turning into a drop at low temperature. To illustrate this, we extrapolate the in-field resistivity $\rho_c(B)$ to $B = 0$ using the same two-band model (electron and hole carriers) that self-consistently accounted for the temperature and field dependence of the longitudinal and transverse (Hall) resistivities of $YBa_2Cu_4O_8$ (Ref. 29). The transverse magnetoresistance can be fitted with a two-band model

$$\rho(B) = \frac{(\sigma_h + \sigma_e) + \sigma_h\sigma_e(\sigma_h R_h^2 + \sigma_e R_e^2)B^2}{(\sigma_h + \sigma_e)^2 + \sigma_h^2\sigma_e^2(R_h + R_e)^2 B^2},$$

$$\rho(B) = \rho_0 + \frac{\alpha B^2}{1 + \beta B^2}, \qquad (1)$$
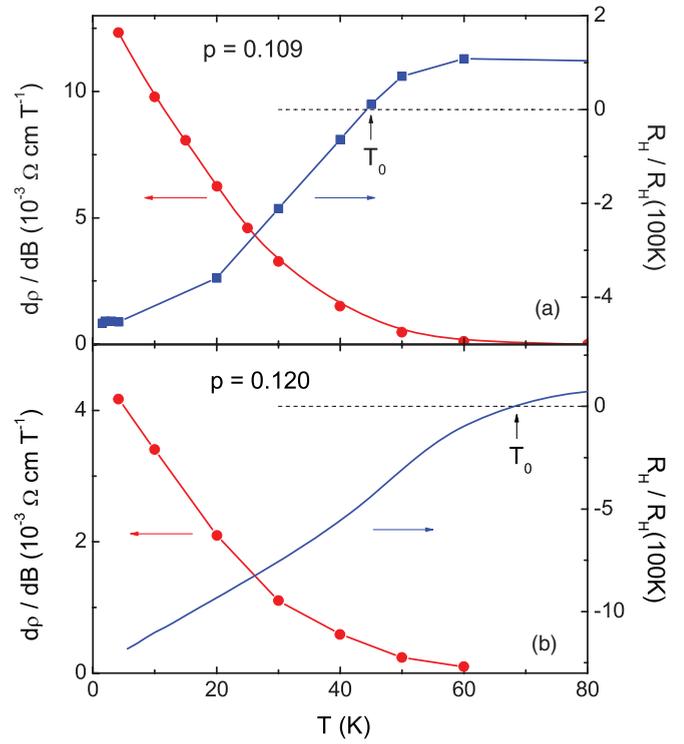
FIG. 5. (Color online) The slope of the *c*-axis magnetoresistance evaluated at $B = 50$ T (red circles; left axis) and in-plane Hall coefficient R_H (blue squares; right axis) of (a) $YBa_2Cu_3O_y$ ($p = 0.109$), (b) $YBa_2Cu_3O_y$ ($p = 0.120$) as a function of temperature. R_H data measured at (a) $B = 54$ T, and (b) $B = 45$ T is taken from Ref. 22 and normalized by its value at $T = 100$ K. T_0 is the temperature at which $R_H(T)$ changes sign from positive at high temperature to negative at low temperature (Refs. 11 and 22).

where σ_h (σ_e) is the conductivity of holes (electrons) and R_h (R_e) is the Hall coefficient for hole (electron) carriers. Using the three free parameters ρ_0, α, and β, we were able to subtract
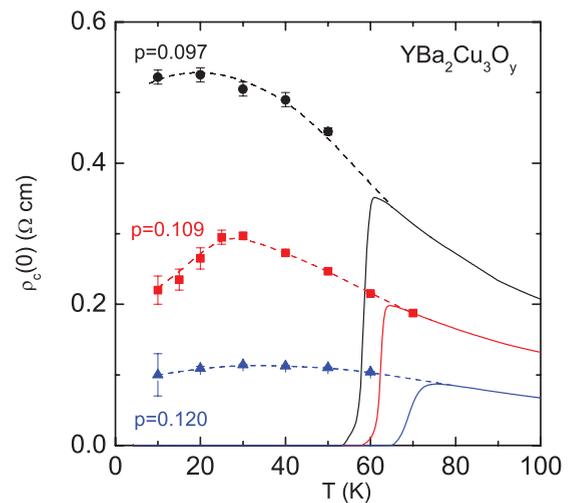
FIG. 6. (Color online) Temperature dependence of the *c*-axis resistivity of $YBa_2Cu_3O_y$ from which the magnetoresistance has been subtracted using a two-band model (see Sec. V) for the three samples, as labeled. Solid lines show the resistivity measured in zero magnetic field. Dashed lines are a guide to the eye.

the orbital magnetoresistance from the field sweeps and get the temperature dependence of the zero-field resistivity $\rho_c(0) = \rho_0(T)$. To estimate error bars we fitted each field sweep data set to Eq. (1) between a lower bound B_{cutoff} and the maximum field strength and monitored the value of $\rho_c(0)$ as a function of B_{cutoff}. The resulting fits to $\rho_c(B)$ down to 10 K for all three samples are shown in thin solid lines in the insets of Fig. 1. They yield the extrapolated zero-field resistivity $\rho_c(0)$ shown in the symbols in Fig. 6. The initial rise in $\rho_c(0)$ with decreasing temperature turns into a drop at low temperature, passing through a maximum at $T_{coh} = 27 \pm 3$ K for the $p = 0.109$ sample. This is in reasonable agreement with the energy scale $t_\perp \approx 15$ K obtained from the splitting of frequencies in quantum oscillations for YBa$_2$Cu$_3$O$_y$ at $p = 0.10$–0.11 (Refs. 18 and 20). The same analysis for the two other compositions yields $T_{coh} = 20 \pm 5$ K for $p = 0.097$ and $T_{coh} = 35 \pm 5$ K for $p = 0.12$.

VI. DISCUSSION

The coherent c-axis transport at low temperature is a direct consequence of the Fermi surface reconstruction occurring at a temperature scale $T_{charge} \approx T_0$. From c-axis transport measurements, we define T_{coh} as the characteristic temperature for the crossover to the coherent regime at which $\rho_c(0)$ peaks (see Fig. 6). In Fig. 7, we compare the temperatures T_{coh} and T_0 as a function of doping on the phase diagram of YBa$_2$Cu$_3$O$_y$. The two phenomena trend similarly as a function of doping, both decreasing to lower T with decreasing p. In addition,
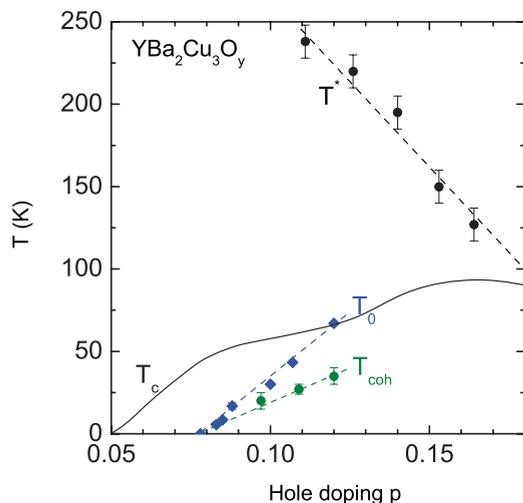
FIG. 7. (Color online) Temperature-doping phase diagram of YBa$_2$Cu$_3$O$_y$, with the superconducting phase in zero magnetic field delineated by the transition temperature T_c. Black circles mark the temperature T^* below which the in-plane resistivity deviates from its linear temperature dependence at high temperature (from data in Ref. 38), a standard definition for the onset of the pseudogap phase. The coherence temperature T_{coh} (green circles) is the temperature where $\rho_c(T)$ peaks (see Fig. 6). The coherence crossover splits the phase diagram into two regions: an incoherent two-dimensional (2D) regime above and a coherent 3D regime below. T_0 is the temperature at which the normal-state in-plane Hall coefficient $R_H(T)$ of YBa$_2$Cu$_3$O$_y$ changes sign from positive at high temperature to negative at low temperature (blue diamonds; from Ref. 22).

these characteristic temperatures extrapolate to zero at lower doping $p \approx 0.08$, where $R_H(T)$ no longer shows any downturn (see data for sample with $T_c = 44.5$ K in Ref. 22). This qualitative change has been attributed to the disappearance of the electron pocket, either caused by a Lifshitz transition[22] or by a phase transition.[30] Earlier measurements of c-axis transport on a sample with $T_c = 49$ K (Ref. 25) are consistent with such a transition: the MR in $\rho_c(T)$ is entirely gone and ρ_c is now incoherent, increasing down to the lowest temperatures.

In the framework of conventional theory of metals, the c-axis conductivity is given by $\sigma_c = \frac{4e^2 c t_\perp^2 m^* \tau_c}{\pi \hbar^4}$ where c is the c-axis lattice parameter, τ_c is the relaxation time, and m^* is the effective mass. For a tetragonal cuprate material and due to the crystallographic structure,[31] the interlayer hopping integral $t_\perp$ depends strongly on the in-plane momentum **k** of carriers, namely[32] $t_\perp(\mathbf{k}) = \frac{t_\perp^0}{4}[\cos(k_x a) - \cos(k_y b)]^2$. It is maximum at the antinode [i.e., at the $(\pi, 0)$ (and equivalent) points in the Brillouin zone]. Between the pseudogap temperature T^* and the temperature characteristic of the FS reconstruction T_0, the insulating-like behavior in ρ_c and the absence of the Drude peak in c-axis optical conductivity measurements in the underdoped regime[9] has been ascribed to the absence of a well-defined quasiparticle peak in the antinodal regions as seen by ARPES measurements.[2]

Below T_0 and for doping levels $p > 0.08$, the field-induced charge stripe order detected by high-field NMR in YBa$_2$Cu$_3$O$_y$ (Ref. 15) causes the reconstruction of the FS at low temperature. The role of the magnetic field is to weaken superconductivity to reveal the competing stripe order. As a consequence, there is no contradiction between the low-temperature/high-field electronic properties of underdoped YBa$_2$Cu$_3$O$_y$ and the FS seen by ARPES at zero field[2] or the absence of a Drude peak at low frequencies at magnetic fields below the threshold field.[33] This FS reconstruction produces a high mobility electron pocket which dominates the in-plane transport properties[22] and is responsible for the c-axis coherence at low temperature.

Taking into account the in-plane momentum dependence of the interlayer hopping integral $t_\perp$, the crossover to the coherent c-axis transport suggests that either some electronic states exist close to the antinode in the Brillouin zone[34–36] or that the reconstructed FS allows for assisted interlayer hopping term through one-dimensional (1D) bands, for example. In the former scenario, strong scattering at $(0, \pi)$ associated with charge fluctuations at a wave vector $Q_x = [\pi/2a, 0]$ softens or freezes out when the charge order sets in at low temperature, restoring coherent quasiparticles close to the antinode. Below a doping level $p < 0.08$, the electron pocket disappears, probably because of a transition from a charge stripe order ($p > 0.08$) to a phase with spin order ($p < 0.08$) (Ref. 37). In the absence of this electron pocket, both in-plane[22] and out-of-plane[25] transport properties are non-metallic-like at low temperature.

*cyril.proust@lncmi.cnrs.fr

[1] T. Timusk and B. Statt, Rep. Prog. Phys. **62**, 61 (1999).

[2] M. R. Norman *et al.*, Nature (London) **392**, 157 (1998).

[3] S. L. Cooper and K. E. Gray, *Physical Properties of High Temperature Superconductors IV* (World Scientific, Singapore, 1994), Vol. IV.

[4] D. G. Clarke and S. P. Strong, Adv. Phys. **46**, 545 (1997).

[5] N. E. Hussey, *Handbook of High-Temperature Superconductivity* (Springer, New York, 2007).

[6] P. W. Anderson, Science **256**, 1526 (1992).

[7] D. B. Gutman and D. L. Maslov, Phys. Rev. Lett. **99**, 196602 (2007).

[8] M. Ferrero, O. Parcollet, A. Georges, G. Kotliar, and D. N. Basov, Phys. Rev. B **82**, 054502 (2010).

[9] D. N. Basov and T. Timusk, Rev. Mod. Phys. **77**, 721 (2005).

[10] N. Doiron-Leyraud *et al.*, Nature (London) **447**, 565 (2007).

[11] D. LeBoeuf *et al.*, Nature (London) **450**, 533 (2007).

[12] J. Chang *et al.*, Phys. Rev. Lett. **104**, 057005 (2010).

[13] F. Laliberté *et al.*, Nature Comm. **2**, 432 (2011).

[14] B. Vignolle *et al.*, Nature (London) **455**, 952 (2008).

[15] T. Wu *et al.*, Nature (London) **477**, 191 (2011).

[16] J. Fink, V. Soltwisch, J. Geck, E. Schierle, E. Weschke, and B. Buchner, Phys. Rev. B **83**, 092503 (2011).

[17] J. M. Tranquada *et al.*, Nature (London) **375**, 561 (1995).

[18] A. Audouard, C. Jaudet, D. Vignolles, R. Liang, D. A. Bonn, W. N. Hardy, L. Taillefer, and C. Proust, Phys. Rev. Lett. **103**, 157003 (2009).

[19] S. E. Sebastian, N. Harrison, P. A. Goddard, M. M. Altarawneh, C. H. Mielke, R. Liang, D. A. Bonn, W. N. Hardy, O. K. Andersen, and G. G. Lonzarich, Phys. Rev. B **81**, 214524 (2010).

[20] B. J. Ramshaw *et al.*, Nat. Phys. **7**, 234 (2011).

[21] S. E. Sebastian, N. Harrison, R. Liang, D. A. Bonn, W. N. Hardy, C. H. Mielke, and G. G. Lonzarich, Phys. Rev. Lett. **108**, 196403 (2012).

[22] D. LeBoeuf *et al.*, Phys. Rev. B **83**, 054506 (2011).

[23] R. Liang *et al.*, Physica C **336**, 57 (2000).

[24] R. Liang, D. A. Bonn, and W. N. Hardy, Phys. Rev. B **73**, 180505(R) (2006).

[25] F. F. Balakirev *et al.*, Physica C **341–348**, 1877 (2000).

[26] N. E. Hussey *et al.*, Nature (London) **425**, 814 (2003).

[27] S. C. Riggs *et al.*, Nat. Phys. **7**, 332 (2011).

[28] N. Harrison and S. E. Sebastian, Phys. Rev. Lett. **106**, 226402 (2011).

[29] P. M. C. Rourke, A. F. Bangura, C. Proust, J. Levallois, N. Doiron-Leyraud, D. LeBoeuf, L. Taillefer, S. Adachi, M. L. Sutherland, and N. E. Hussey, Phys. Rev. B **82**, 020514(R) (2010).

[30] S. E. Sebastian *et al.*, Proc. Natl. Acad. Sci. USA **107**, 6175 (2010).

[31] O. K. Andersen *et al.*, J. Phys. Chem. Solids **56**, 1573 (1995).

[32] S. Chakravarty *et al.*, Science **261**, 337 (1993).

[33] J. M. Tranquada, D. N. Basov, A. D. LaForge, and A. A. Schafgans, Phys. Rev. B **81**, 060506(R) (2010).

[34] A. J. Millis and M. R. Norman, Phys. Rev. B **76**, 220503(R) (2007).

[35] S. Chakravarty and H.-Y. Kee, Proc. Natl. Acad. Sci. USA **105**, 8835 (2008).

[36] H. Yao, D. H. Lee, and S. Kivelson, Phys. Rev. B **84**, 012507 (2011).

[37] D. Haug *et al.*, New J. Phys. **12**, 105006 (2010).

[38] Y. Ando, S. Komiya, K. Segawa, S. Ono, and Y. Kurita, Phys. Rev. Lett. **93**, 267001 (2004).